

## I. SUPPLEMENTARY RESULTS

We have decided to provide additional results for reviewers in this supplementary document in order to demonstrate versatility of the proposed multichannel blind deconvolution (MCBD) algorithm. We believe these results are not directly necessary for understanding the proposed method and we also wanted to avoid a lengthy manuscript. First we show the influence of the positivity constraint and  $\mathbf{R}_\Delta$  on synthetically blurred data. Second we provide results of blind deconvolution on Levin's data set [1] and other real digital photos.

The setup for the synthetic data experiment was the same as described in the manuscript. We took the Lena image, Fig. 1(a), and convolve it with two  $9 \times 9$  blurs, Fig. 1(b), and add noise at three different levels,  $\text{SNR} = 50, 30, 10\text{dB}$ . An example of blurry images for the least noisy case is in Fig. 1(c). To evaluate performance in every iteration  $j$  of the main loop, we use *normalized root mean square error* defined as  $\text{NRMSE} = \|\hat{\mathbf{h}}^j - \mathbf{h}^*\| / \|\mathbf{h}^*\|$ , where  $\hat{\mathbf{h}}^j$  is the estimation of PSFs after  $j$  iterations and  $\mathbf{h}^*$  are the true PSFs. NRMSE as a function of iterations and estimated PSFs for different situations are summarized in a  $3 \times 3$  table in Fig. 2. NRMSE is plotted in logarithmic scale. Three rows correspond to three SNRs and three columns to different added features of the algorithm. Column (a) shows results in the case both the positivity constraint and  $\mathbf{R}_\Delta$  are used. Column (b) shows results in the case positivity is used, but instead of the proposed  $\mathbf{R}_\Delta$ , the original MC constraint  $\mathbf{R}$  is used. The final column (c) corresponds to the case positivity is not enforced in the algorithm. In each case we ran the algorithm with three different PSF supports:  $9 \times 9$  (solid line),  $15 \times 15$  (dotted line) and  $21 \times 21$  (dashed line). The corresponding estimated sharp images for PSF support  $21 \times 21$  are summarized in Fig. 3. One can see that the proposed MCBD method, column (a), provides accurate results regardless of the degree of PSF size overestimation and shows good stability with respect to noise.

There are several interesting points we can draw from the obtained results. First of all, the mean square error (MSE) decreases very quickly. In most of the cases, after 5 iterations MSE remains almost constant. For overestimated blur supports (dotted and dashed line) MSEs are higher than for the correct blur support (solid line). This is logical, since in the overestimated case the dimensionality of the problem is higher and the MC constraint  $\mathbf{R}$  is less effective as discussed in Sec. IV-C. of the original manuscript. The smallest difference between the overestimated and correct support is in the case of  $\mathbf{R}_\Delta$  (column a). The largest difference is in the case positivity is not enforced (column c). We see that positivity is important in order to obtain a stable solution if the blur support is not known. The estimated PSFs are erroneous (see for example 1c for  $21 \times 21$ ) and the corresponding estimated images exhibit profound

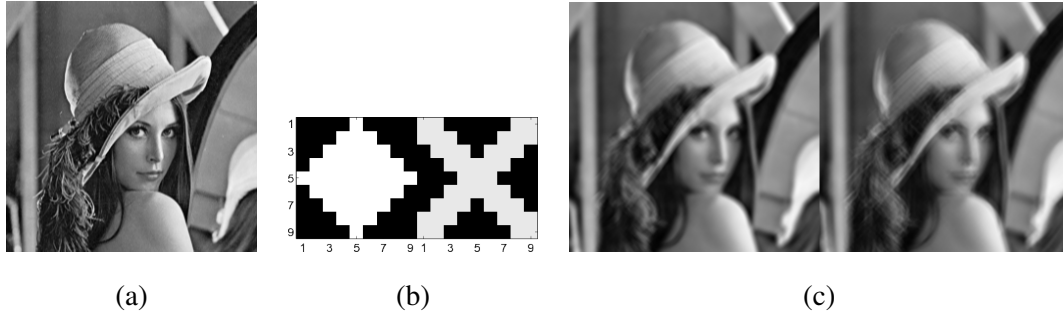


Fig. 1. Test data set: (a) original image  $256 \times 256$ , (b) two blurs  $9 \times 9$ , (c) example of an input blurry pair with  $\text{SNR} = 50\text{dB}$ .

artifacts as shown in Fig. 3, 1c and 2c in the last column.

Clearly, as the noise level increases (from row 1 to row 3), the lowest attainable MSE increases. For  $\text{SNR} = 50\text{dB}$  (row 1), estimated PSFs are very accurate and there is not much difference between  $\mathbf{R}_\Delta$  (1a) and  $\mathbf{R}$  (1b). The corresponding estimated images (1a) and (1b) shown in Fig. 3 are very similar indeed. However for higher noise levels  $\text{SNR} = 30\text{dB}$ ,  $\mathbf{R}_\Delta$  (2a) produces more accurate estimates compare to  $\mathbf{R}$  (2b). The estimated image (2b) contains artifacts, whereas (2a) is still artifact free. This observation is in line with our discussion in Sec. IV-B. of the original manuscript. As the noise level increases further to  $\text{SNR} = 10\text{dB}$ , superiority of  $\mathbf{R}_\Delta$  (3a) is less evident, since the image corruption by noise is too severe (see an example of an input image in Fig. 3, row 3). Nevertheless, PSF shapes are most recognizable in the case of  $\mathbf{R}_\Delta$  (3a). However, reconstructed images (row 3 in Fig. 3) look very similar as TV regularization takes over.

We further tested the proposed MCB algorithm on Levin’s data set. This database contains images blurred by real camera shake. There are 4 different images labeled 5 to 8 and 8 different blurs labeled 1 to 8, having 32 blurred images in total. The original sharp images together with PSFs obtained from images of bright dots are also included in the data set for evaluation purposes. We split the blurred images into groups of 4 and applied our MCB algorithm on each quad. The results of all 8 experiments are summarized in Figs. 4 to 11. One can see that the estimated blurs are very similar to the “ideal” ones and that the estimated sharp images are almost perfect in all 8 cases.

Additional results of blind deconvolution of large photos and blurs obtained by a digital camera are given in Figs. 12 and 13.

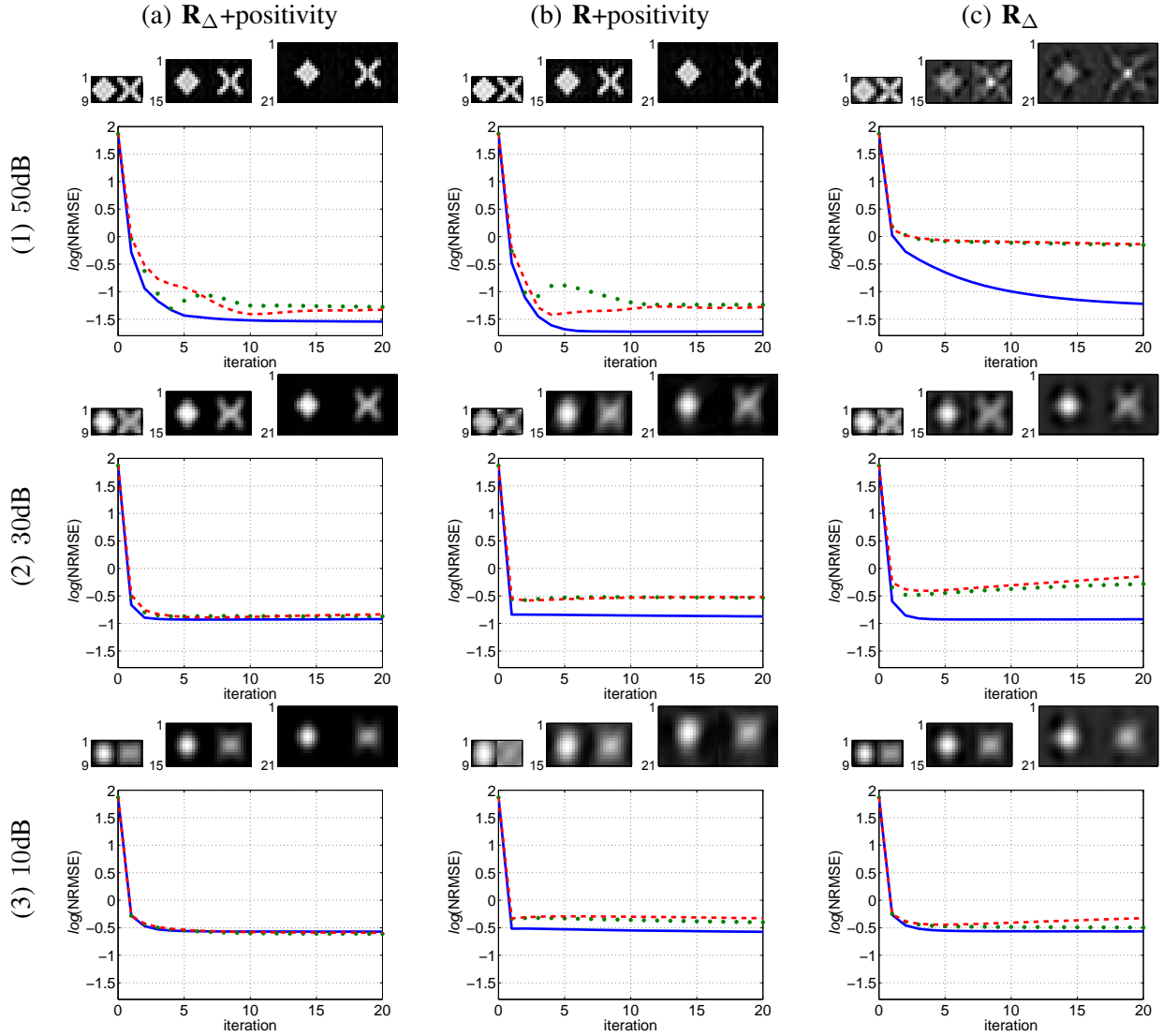


Fig. 2. Estimated PSFs and plots of normalized root mean square error arranged in a  $3 \times 3$  table. Rows 1 to 3 correspond to different noise levels in input blurry images: (1) 50dB, (2) 30dB, (3) 10dB. Columns (a) to (c) correspond to different added features of the proposed algorithm: (a)  $\mathbf{R}_\Delta$  and positivity constraint, (b)  $\mathbf{R}$  and positivity constraint, (c)  $\mathbf{R}_\Delta$  and no positivity constraint. Three different PSF supports were considered in each case: correct PSF size  $9 \times 9$  (solid line), and two overestimated sizes  $15 \times 15$  (dotted line) and  $21 \times 21$  (dashed line).

## REFERENCES

- [1] A. Levin, Y. Weiss, F. Durand, and W. Freeman, "Understanding and evaluating blind deconvolution algorithms," in *Proc. IEEE Conference on Computer Vision and Pattern Recognition CVPR '09*, 2009.

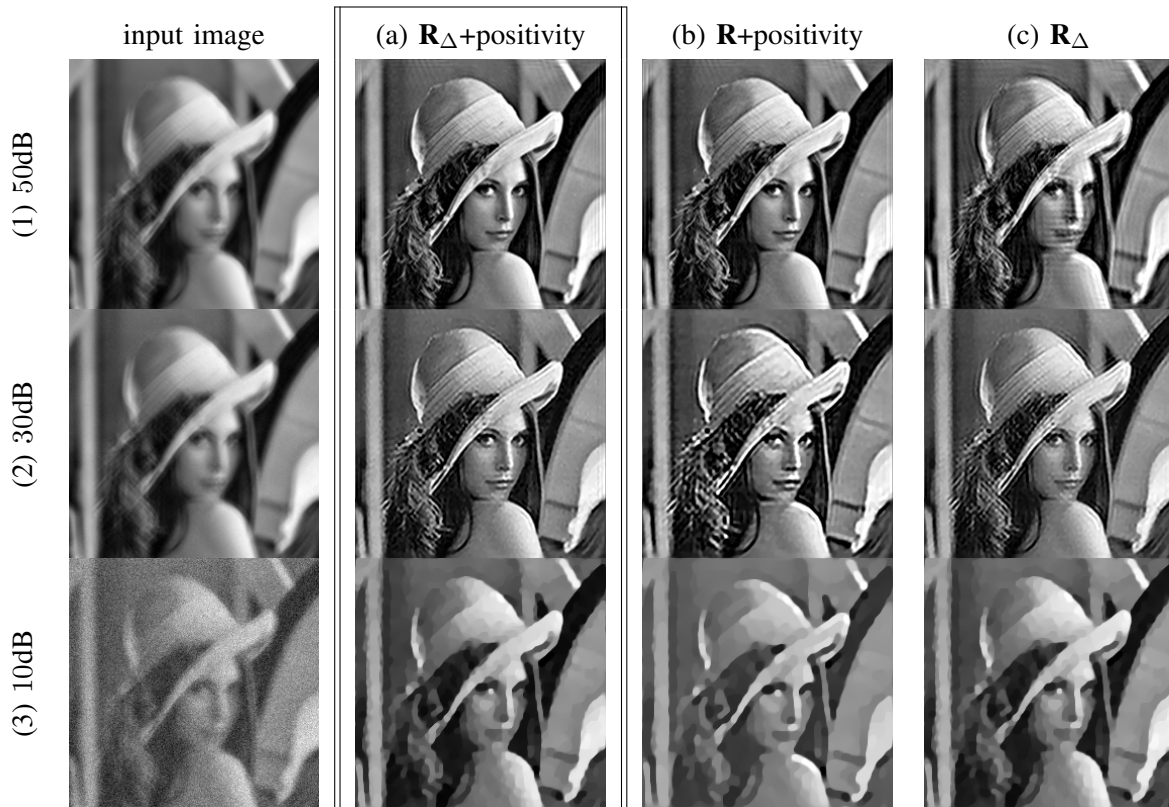


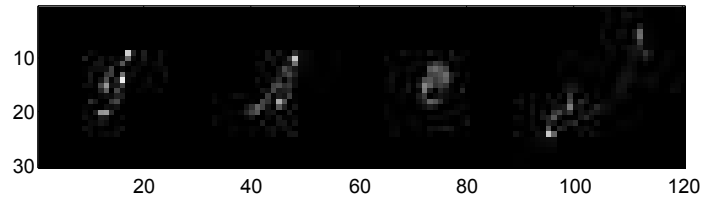
Fig. 3. Estimated sharp images for PSFs of size  $21 \times 21$ . Images follow the same arrangement as in Fig. 2 where in the first column we show the second blurred image from each pair. The framed column (a) contains results of our proposed method.



(a) acquired blurred images



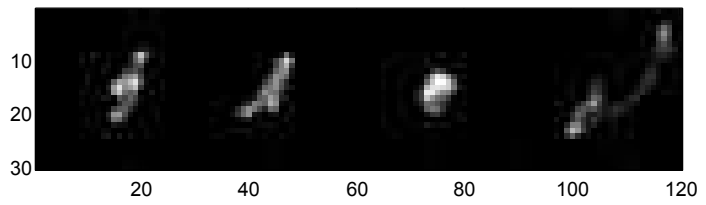
(b) original image



(c) original PSFs

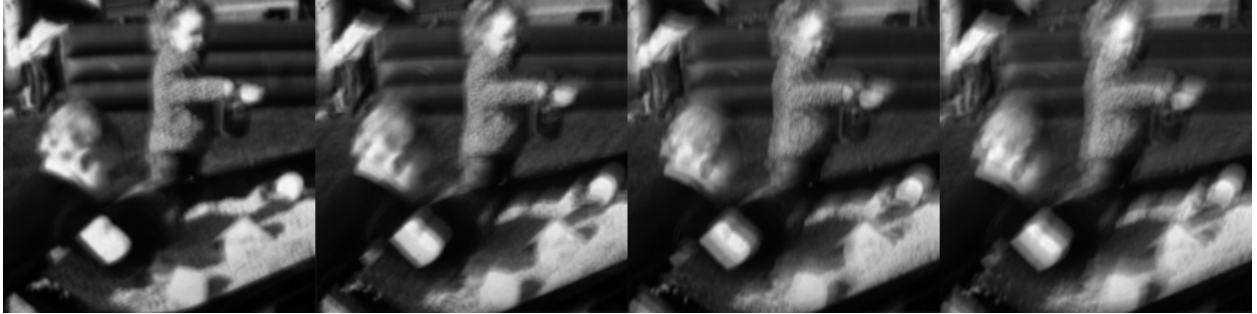


(d) estimated image



(e) estimated PSFs

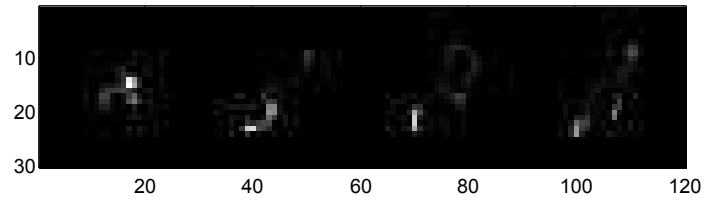
Fig. 4. Levin's data set, Image 5, PSFs 1-4: (a) four blurred images acquired with a shaking camera, (b) image captured with a still camera, (c) ideal PSFs obtained as images of a bright spot, (d) sharp image estimated with our MC method, and (e) PSFs estimated with our MC method.



(a) acquired blurred images



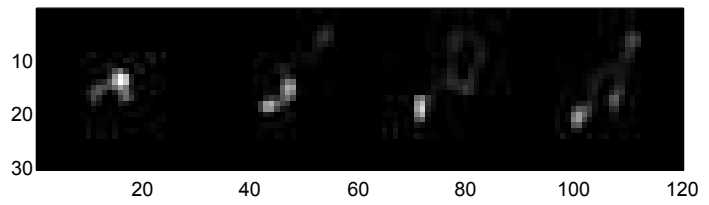
(b) original image



(c) original PSFs



(d) estimated image



(e) estimated PSFs

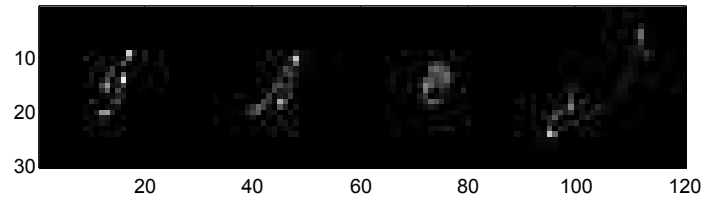
Fig. 5. Levin's data set, Image 5, PSFs 5-8: (a) four blurred images acquired with a shaking camera, (b) image captured with a still camera, (c) ideal PSFs obtained as images of a bright spot, (d) sharp image estimated with our MC method, and (e) PSFs estimated with our MC method.



(a) acquired blurred images



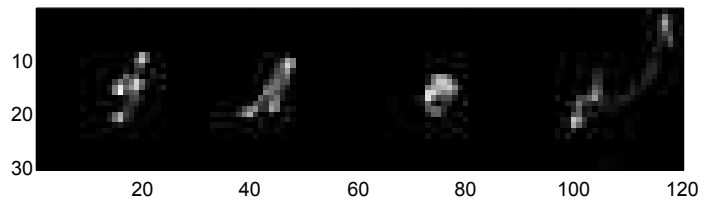
(b) original image



(c) original PSFs



(d) estimated image



(e) estimated PSFs

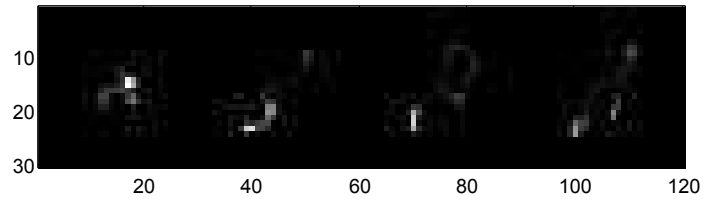
Fig. 6. Levin's data set, Image 6, PSFs 1-4: (a) four blurred images acquired with a shaking camera, (b) image captured with a still camera, (c) ideal PSFs obtained as images of a bright spot, (d) sharp image estimated with our MC method, and (e) PSFs estimated with our MC method.



(a) acquired blurred images



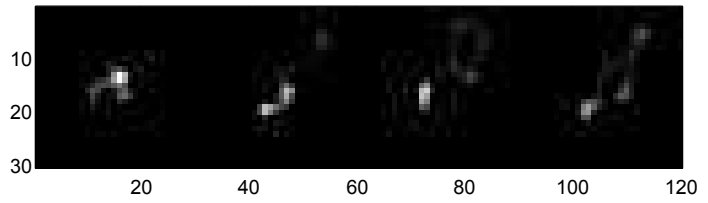
(b) original image



(c) original PSFs



(d) estimated image



(e) estimated PSFs

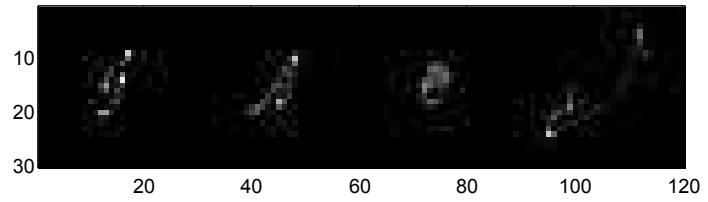
Fig. 7. Levin's data set, Image 6, PSFs 5-8: (a) four blurred images acquired with a shaking camera, (b) image captured with a still camera, (c) ideal PSFs obtained as images of a bright spot, (d) sharp image estimated with our MC method, and (e) PSFs estimated with our MC method.



(a) acquired blurred images



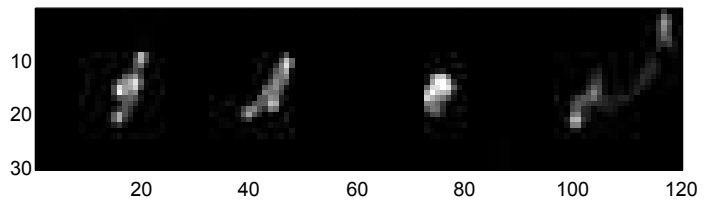
(b) original image



(c) original PSFs

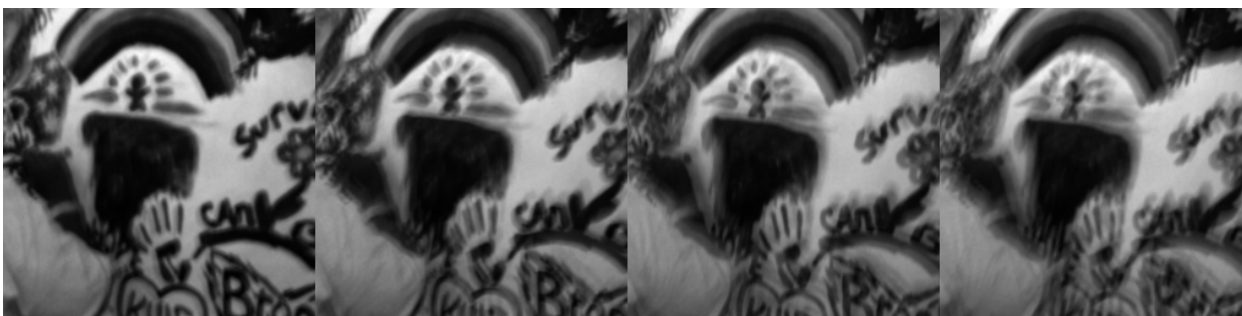


(d) estimated image



(e) estimated PSFs

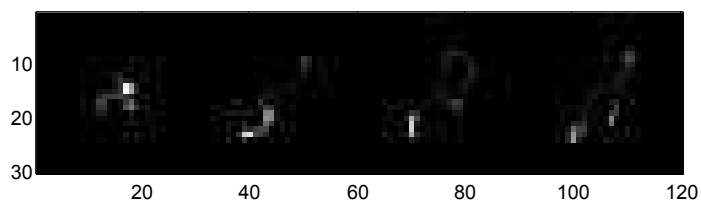
Fig. 8. Levin's data set, Image 7, PSFs 1-4: (a) four blurred images acquired with a shaking camera, (b) image captured with a still camera, (c) ideal PSFs obtained as images of a bright spot, (d) sharp image estimated with our MC method, and (e) PSFs estimated with our MC method.



(a) acquired blurred images



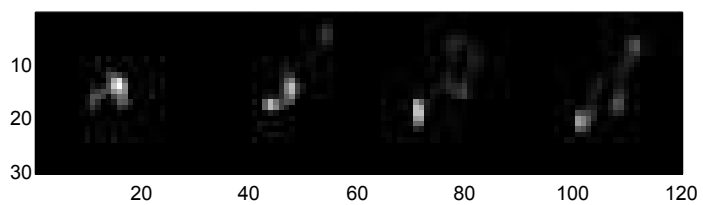
(b) original image



(c) original PSFs

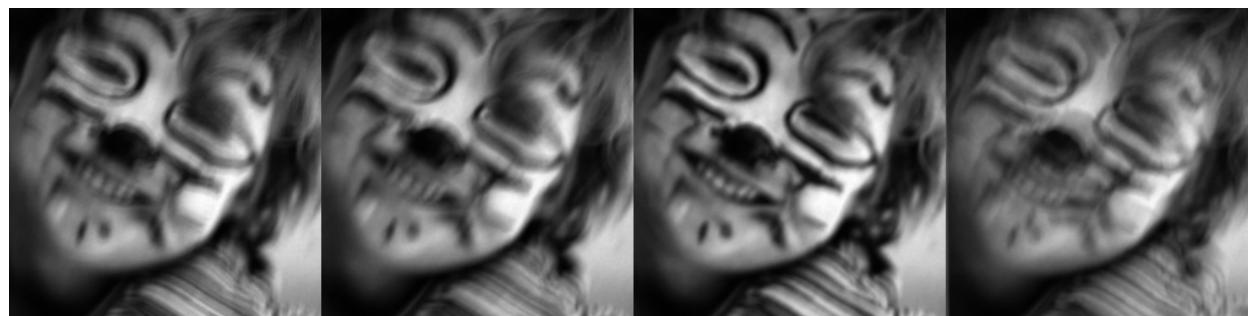


(d) estimated image



(e) estimated PSFs

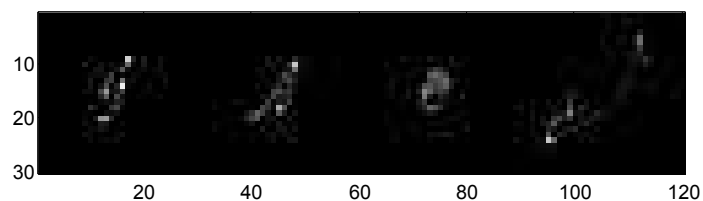
Fig. 9. Levin's data set, Image 7, PSFs 5-8: (a) four blurred images acquired with a shaking camera, (b) image captured with a still camera, (c) ideal PSFs obtained as images of a bright spot, (d) sharp image estimated with our MC method, and (e) PSFs estimated with our MC method.



(a) acquired blurred images



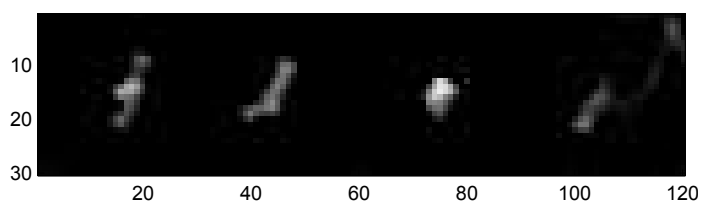
(b) original image



(c) original PSFs

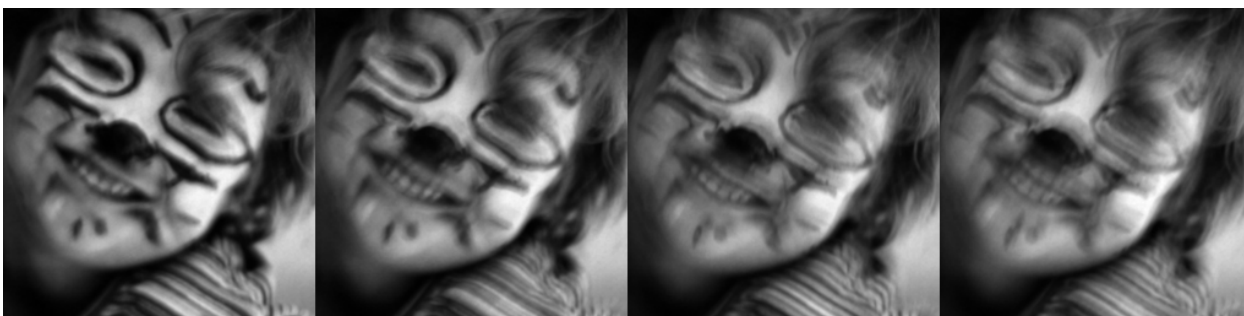


(d) estimated image



(e) estimated PSFs

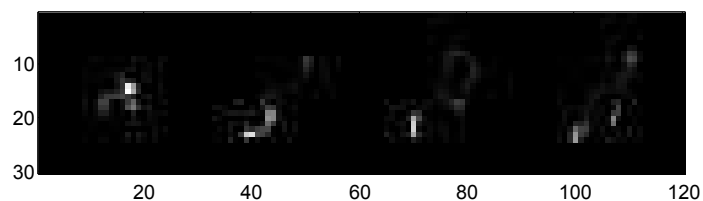
Fig. 10. Levin's data set, Image 8, PSFs 1-4: (a) four blurred images acquired with a shaking camera, (b) image captured with a still camera, (c) ideal PSFs obtained as images of a bright spot, (d) sharp image estimated with our MC method, and (e) PSFs estimated with our MC method.



(a) acquired blurred images



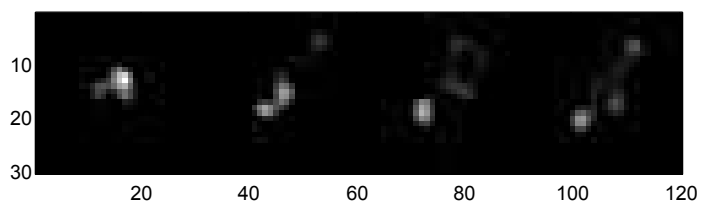
(b) original image



(c) original PSFs



(d) estimated image



(e) estimated PSFs

Fig. 11. Levin's data set, Image 8, PSFs 5-8: (a) four blurred images acquired with a shaking camera, (b) image captured with a still camera, (c) ideal PSFs obtained as images of a bright spot, (d) sharp image estimated with our MC method, and (e) PSFs estimated with our MC method.

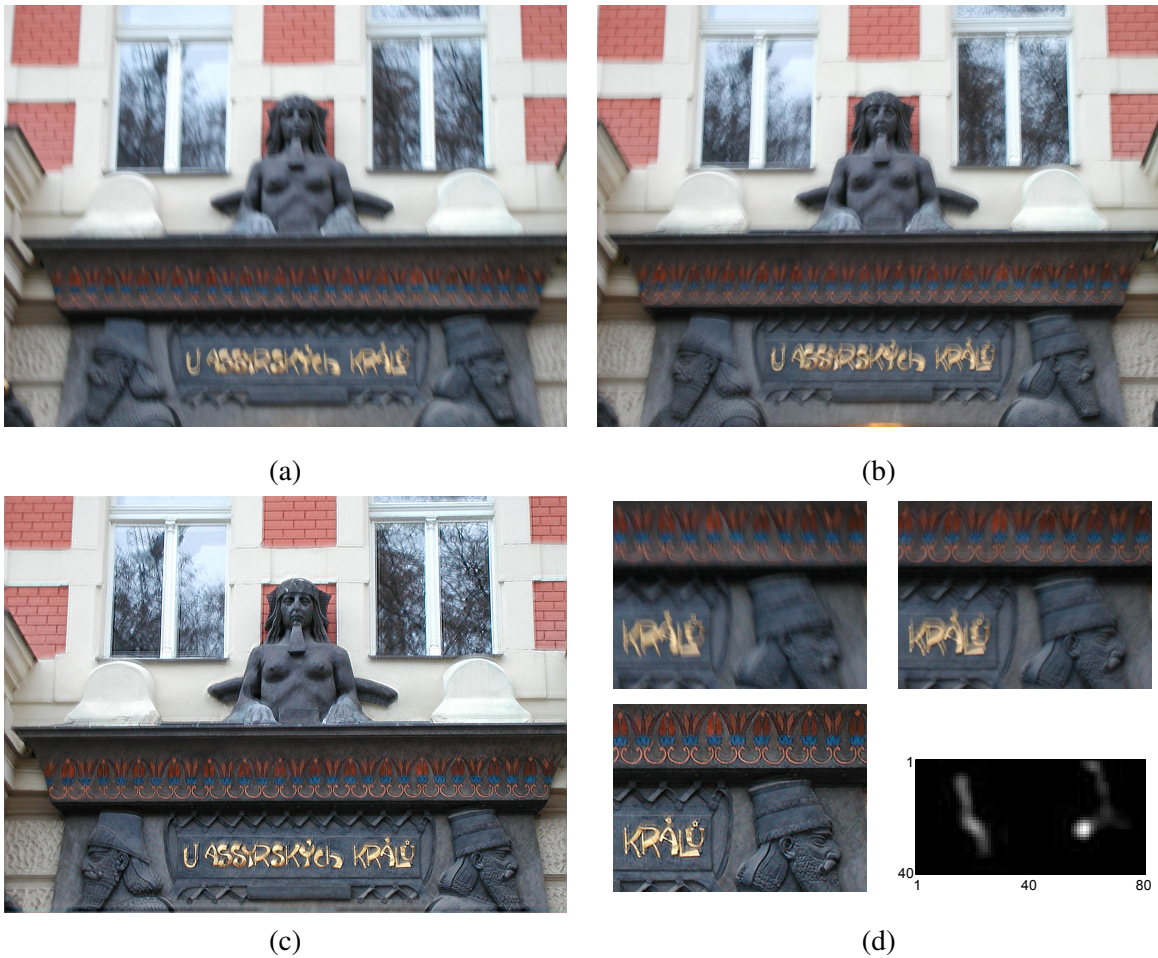
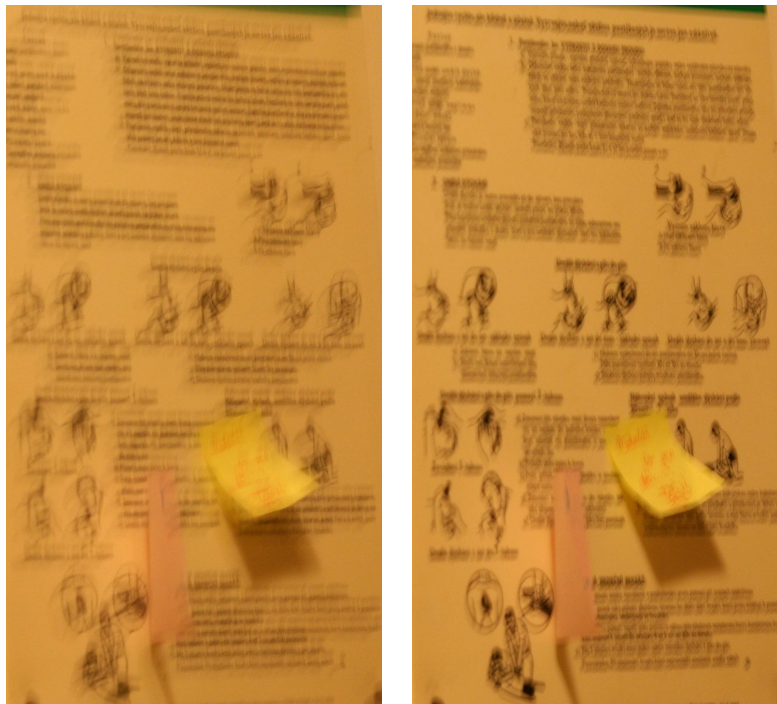


Fig. 12. Real data set: (a) - (b) two input blurry images of size  $2048 \times 1536$ , (c) estimated output sharp image using the proposed algorithm, (d) close-ups of the input images and the output, and estimated PSFs of size  $40 \times 40$ .



(a)

(b)



(c)



(d)

Fig. 13. Real data set: (a) - (b) two input blurry images of size  $1600 \times 1800$ , (c) estimated output sharp image using the proposed algorithm, (d) close-ups of the input images and the output, and estimated PSFs of size  $60 \times 60$ .